Published by :
http://www.ijert.org

International Journal of Engineering Research & Technology (IJERT)
ISSN: 2278-0181
Vol. 8 Issue 06, June-2019

Effect of Layers Thickness and Temperature on Electronic Transport of Nanostructures Infrared Detectors

Nassima Benchtaber, Abdelhakim Nafidi, Samir Melkoud, Meriem Benaadad, Driss Barkissy
Laboratory of Condensed Matter Physics and Nanomaterials for Renewable Energy
Department of Physics Faculty of Sciences Ibn Zohr University
Agadir, Morocco

***Abstract*— We report here the effect of layers thickness and temperature on electronic transport of nanostructure by calculation of band structure of two superlattices SL_1 InAs(d_1)/Gasb(d_2) of type II and SL_2 HgTe/CdTe of type III for infrared detection application. These studies were done using the envelope function formalism. We calculated the energy of carriers as a function of layers thickness, the ration d_1/d_2 and the temperature. The calculated density of states and Fermi level energy shows that temperature generated transitions from quasi bidimensional (Q2D) to three dimensional (3D) in the two SL. The later occurred near 20 K in the p type SL1 and near 84 K in SL2 with p type to n type conductivity transition. We found that these SL are mid infrared and terahertz detectors. The electronic transport parameters calculated here are necessary for the design of infrared photo-detectors.**

Keywords—Superlattices nanostructures; mid infrared detector; density of state; semiconductors; band structures.

I. INTRODUCTION

Infrared detection can be used in a wide range of areas, including remote sensing, astronomy, medicine, surveillance and defense ... Many of these applications, require high sensitivity on a specific band of wavelengths, use infrared systems based on semiconductors [1].

The requirements of the next generation of infrared systems, which are mainly high performance, large bay sizes and high temperature operation, have led to intensive research in industry and academia [2]. This, coupled with the continued development of new growth technologies, has encouraged researchers to study alternative materials suitable for these infrared systems [3].

The infrared detectors based materials are III-V and II-VI semiconductors, The objective of this paper is to study the two type of theses materials superlattice type II (SL_1) wich was Proposed by Mailhiot and Smith [4] in 1987, InAs / GaSb is a stress layer system with Type II band alignment, in which the InAs conduction band is located under the GaSb valence band. As a result, the super-network may have a smaller band gap than any of its components [5]. Electrons and holes tend to reside in different places; electron layers in InAs,and holes in GaSb. And the superlattice type III (SL_2) The peculiarity of this type of superlattice is related to the inversion of light particle bands in HgTe compared to that of CdTe [6]. The energy difference of the peaks of the heavy-hole bands, estimated to be zero [7] but found to be as low as 40meV by magneto-optical measurements [8].

In order to determine the effect of layers thickness and temperature on electronic band structure of these superlattices we have calculated the band structure, band gap energy , the cutoff wavelength and the density of state and we found that SL_1 and SL_2 are mid infrared detector materials.

II. THEORY OF BAND STRUCTURE

The dispersion relation for electrons, light and heavy holes bands is written as [9,10]:

$$\cos = [k_z(d_1 + d_2)] = \cos(k_1 d_1)\cos(k_2 d_2) - \frac{1}{2}[(\xi + \frac{1}{\xi}) + \frac{k_p^{\,2}}{4k_1 k_2}(r + \frac{1}{r} - 2)]\sin(k_1 d_1)\sin(k_2 d_2) \quad (1)$$

With k_z and $k_p(k_x,k_y)$ the wave vector in the growth direction and in-plane of the superlattice and 1, 2 refet to the layers of the SL.

The two samples studied here are SL_1 InAs(d_1=21 Å)/GaSb(d_2=24 Å) and SL_2 HgTe (d_1= 45 Å)/ CdTe(d_2=48 Å) with periods d= d_1+d_2= 45 Å and 93 Å and the ratio d_1/d_2= 0,875 and 0,9375, respectively. So the period of SL_2 is the double of that of SL_1 with the same ratio d_1/d_2 near 0.9.

III. RESULTS AND DISSCUSSION

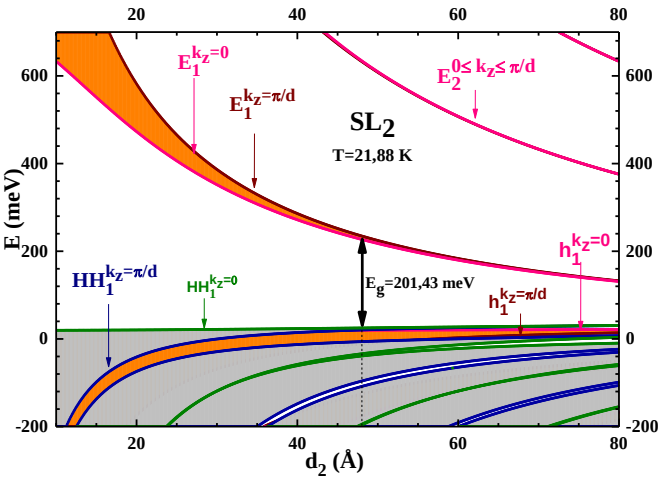

Figure 1: Calculated bands energy of electrons (E_i), heavy-hole (HH_i), and light-hole (h_i) subbands calculated at 21.88 K, in the first Brillouin zone as a function of the barrier thickness d_2 of (CdTe).

International Journal of Engineering Research & Technology (IJERT)
ISSN: 2278-0181
Vol. 8 Issue 06, June-2019

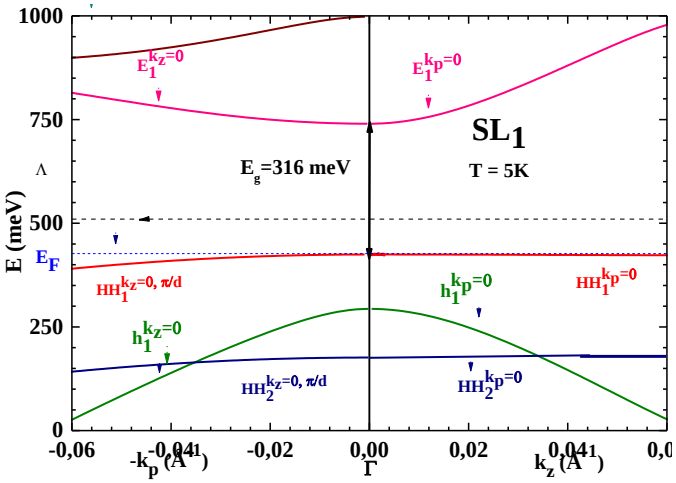

Figure 2. Band structures of the SL_1 along the k_z and k_p directions at 5 K

This study is done using the envelope function formalism and a various parameters like valence band offset, Kane matrix elements and effective masses of the layers.

Figure 1 show the band structure of the SL_2. We plotted the energy as function of layer thickness d_2 of the barrier CdTe. We found that if d_2 increases the width of the bands and the band gap deceases. Our theoretical band gap energy is $E_g=E_1-HH_1$= 201.43 meV at 21.88 K.

Figure 2 shows the calculated band structure of SL_1 along the wave vectors k_z and k_p directions at the T=5K. This SL1 is semiconductor type p with a positive band gap energy E_g=316 meV. Along k_p the first conduction sub-band E_1 and first light hole suband h_1 increases with k_p. whereas HH_1 and HH_2 decreases. Along k_z, the observed week widths of subands (7.5 meV for E_1, 6.4 meV for HH_1 and 8 meV for h_1) indicated a week coupling between the HgTe quantum wells. So, the parallel electronic transport governs in the plane of this superlattice.

The band gap energy E_g as function of the temperature for SL_1 and SL_2 is shown in Figure. 3 (a). When the temperature increases the energy band gap decreases for SL_1 and increases for SL_2.

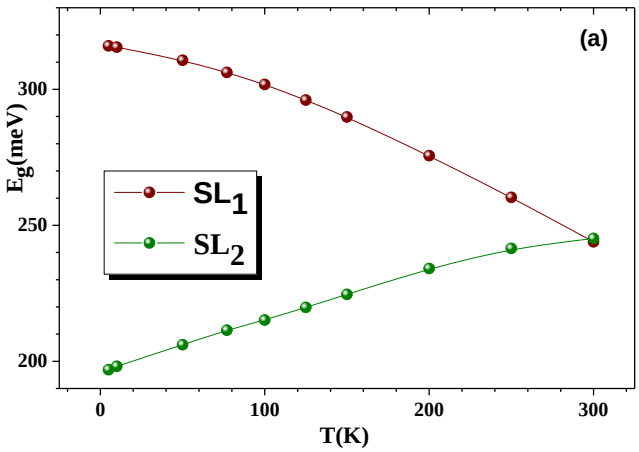

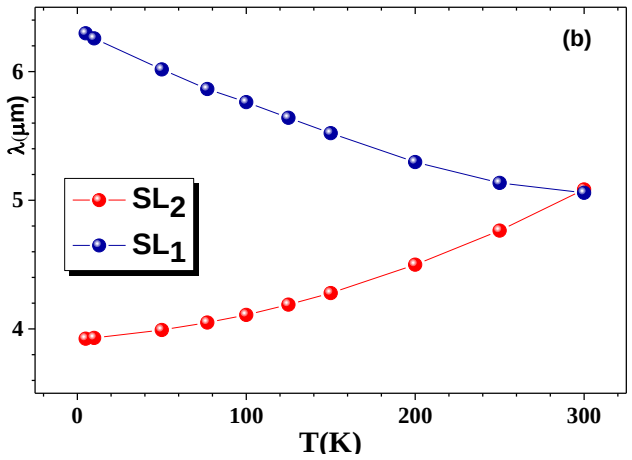

Figure 3. (a) Band gap energy of the SL_1 and SL_2 as function of temperature (b) the cutoff wavelength of the two samples SL_1 and SL_2 as function of temperature.

In figure 3 (b) we have calculated the cutoff wavelength for the SL_1 and SL_2, using the following formulate [11-12]:

$$\lambda_c(nm) = \frac{1240}{E_g(eV)} \qquad (2)$$

We found that when the temperature increases the cut off wavelength of SL_1 decreases and that of the SL_2 increases.

In order to test the effect of layer thickness on the band structure we have calculated and plotted the energy band gap as a function of layer thickness at three temperature (5,77 and 300K) for SL_1 Figure 4 (a) and (21.9,150 and 300k) for SL_2 respectively Figure 4 (b).

We found that for SL_1 at fixed temperature and if the thickness d_2 increases E_g decreases goes to zero and became negative accusing transition conductivity from semiconductor to semi metal. When the temperature increases, at given d_2 the gap decreases and the critical thickness of the transition goes to higher d_{2c}.

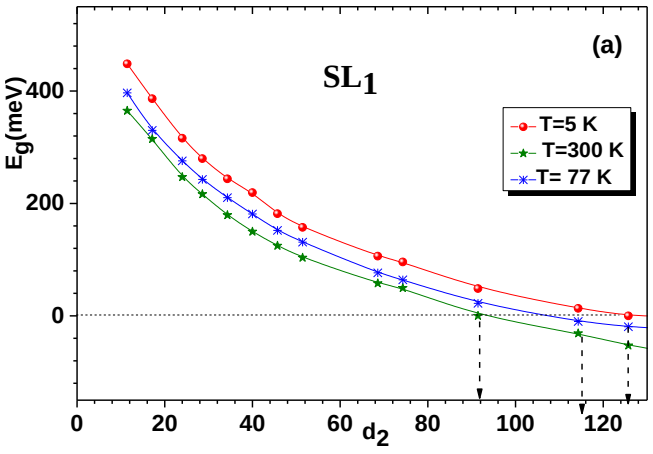

International Journal of Engineering Research & Technology (IJERT)
ISSN: 2278-0181
Vol. 8 Issue 06, June-2019

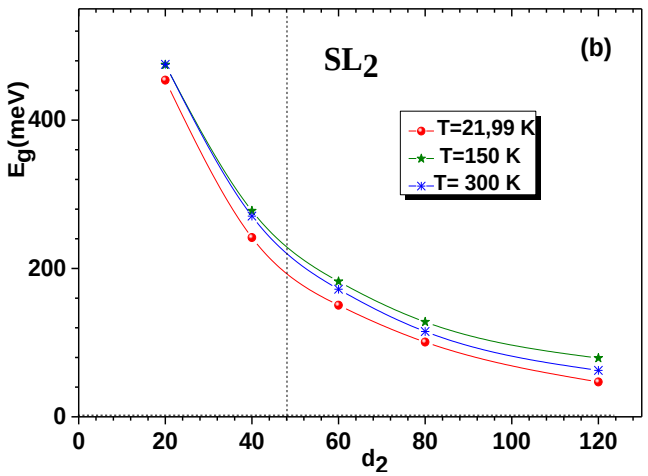

Fig.4. (a) E_g as a function of d_2 at three temperatures SL_1 (T=5, 77 and 300K) (b) E_g as a function of d_2 at three temperatures SL_2 (T=21.99, 150 and 300K)

The SL_2 is semiconductor with gap energy positive. At fixed temperature when d_2 increases the energy band gap decreases.

Our calculated band gap is 316 meV in agreement with the measured 300 meV for SL_1 in [16]. In the SL_2 the observed E_g = 244.1 meV of f H.S. Jung et al. [17] is in good agreement.

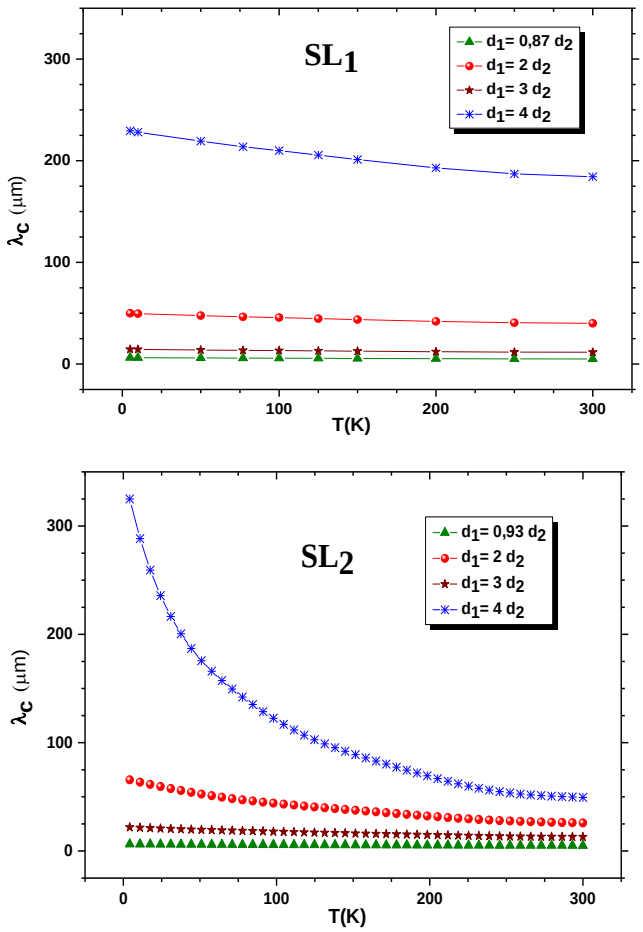

Figure 5: (a) The cut-off wavelength λ_c as function of the temperature for various d_1/d_2 in the SL_1. (b) The cut-off wavelength λ_c as function of the temperature for various d_1/d_2 in the SL_2

with our calculated band gap E_g(300 K) = 245.15 meV.

In figure 5 (a) the cut off wavelength λ_c decreases when the temperature increases and for a given temperature it decreases when d_1/d_2 increases.

In figure 5 (b) the cut off wavelength λ_c decreases when the temperature increases and for a given temperature it decreases when d_1/d_2 increases. In the investigated temperature range of 4.2 K to 300 K, 5060 nm $\leq \lambda_c \leq$ 6300 nm, situates this sample in the mid infrared region.

The effective masse is obtained by the expression below [13]:

$$(\frac{1}{m^*})_{ij} = \frac{1}{\hbar^2}\frac{\partial^2 E_{k_{ij}}}{\partial k_i \partial k_j}, \quad (3)$$

The second derivation of Figure 2 along k_p allow us the determination of the effective masse at the Fermi wave vector k_F.

For the determination of the dimensionality of the carriers charges in the SL we calculated the superlattice i^{th} mini-band, with an energy width $\Delta E = E^i_{max} - E^i_{min}$, the density of states (DOS) can be written as [14,15]:

$$\rho^i_{DOS}(E) = \begin{cases} 0 & \text{for } E^i_{min} > E > E^i_{max} \\ \frac{m^*}{\pi^2\hbar^2} k_z(E) & \text{otherwise} \end{cases} \quad (4)$$

The summation of Eq.(4) gives the total density of states as:

$$\rho_{DOS}(E) = \sum \rho^i_{DOS}(E) \quad (5)$$

Figure 6 shows the calculated density of states versus energy for E_1, HH_1 and h_1 mini-bands at 21.9 K for the SL_2. At 21.88K, the Fermi level energy is on HH_1 so the conductivity is quasi-bidimensional.

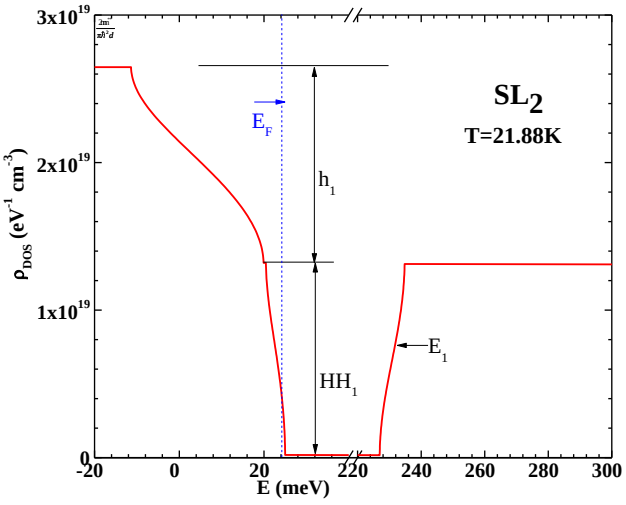

Figure 6: Density of State of the investigated superlattice SL_2 at T=21.88K.

International Journal of Engineering Research & Technology (IJERT)
ISSN: 2278-0181
Vol. 8 Issue 06, June-2019

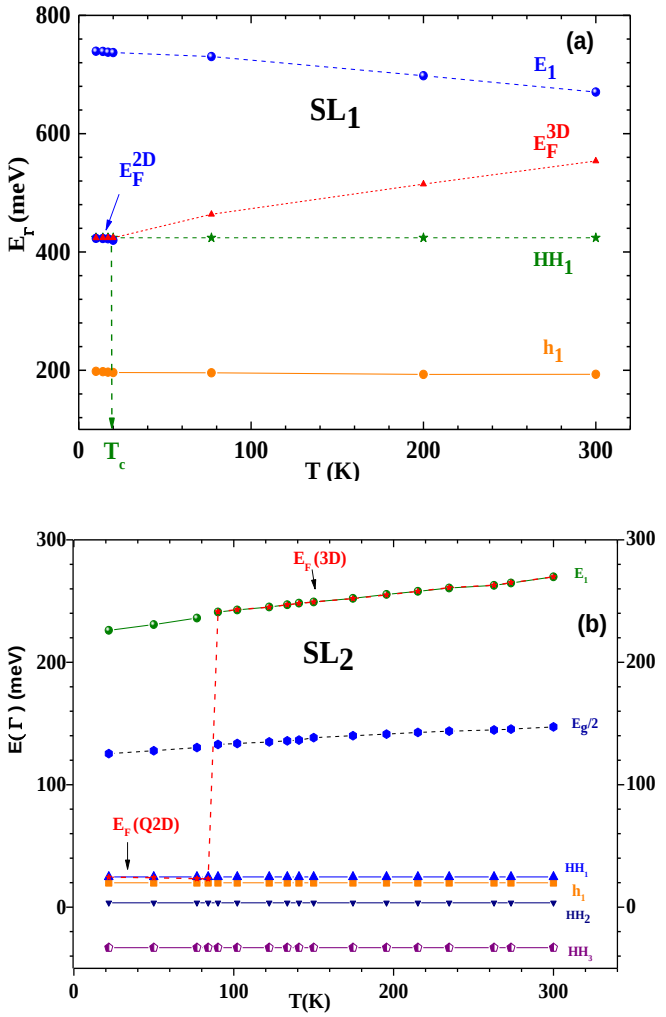

Figure 7: (a) The subbands energy at Γ as a function of temperature and Fermi level energy transition from 2D to 3D for SL_1 and (b) from 2D to 3D for SL_2.

We calculated the Fermi levels using the following formulate in the SL_1

$$E_F = E_{HH1} + \frac{\hbar^2 (k_F^i)^2}{2m^*_{HH1}} \quad (6)$$

with $k_F^{2D} = (2\pi p)^{1/2}$ and $k_F^{3D} = (3\pi^2 p)^{1/3}$

and in the SL_2:

$$\begin{cases} E_{HH1} - E_F = \dfrac{\hbar^2 k_{F2D}^2}{2m^*_{HH1}} \text{ with } k_{F2D} = (2\pi p)^{1/2} \text{ for p type} \\ E_F - E_{HH1} = \dfrac{\hbar^2 k_{F3D}^2}{2m^*_{E1}} \text{ with } k_{F3D} = (3\pi^2 n)^{1/3} \text{ for n type} \end{cases} \quad (7)$$

As chown in figure 7 (a) the sub-bands energy at Γ as a function of temperature and Fermi level transition from 2D to 3D of the sample SL_1. We found that k_{F2D} and k_{F3D} are bi-dimensional and tridimensional Fermi wave vector respectively. When the temperature increases, the Fermi level energy is constant (bi-dimensional gas) until T_c= 22 K. After it increases accusing a tridimensional holes gaz.

Figure 7 (b) shows that the position of the Fermi level energy E_F, indicate p type and quasi bidimentional (Q2D) holes gas at 21.9 K. A similar Figure, at 300 K, showed n type and 3D electrons gas in the investigated superlattice.

At T_{inv}= 84 K, the conductivity of this semiconductor sample change from p-type at low temperatures to n-type at high temperatures. Using the calculated effective mass and the concentrations of electrons from [16], the energy of Fermi level E_F is constant for $T < T_{inv}$ and increases linearly at high temperatures. These means a transition of the carriers charges from quasi bidimensional to three-dimensional.

Our calculated gaps are in agreement with photoluminescence and transport measurements of H. J. Haugan et al. [16] and with H.S. Jung et al. [17].

IV. CONCLUSION

We investigate the effects of layers thickness and temperature on the electronic band structures and transport parameters in two nanostructure superlattice type II and type III. We have calculated the energy band gap; the effective masses the density of state and the Fermi level. We deduce the variation of the band gap and the cut-off wavelength as a function of the temperature and d_1/d_2. We calculated the density of states and the Fermi level as a function of temperature. We found that temperature generated transitions from quasi bidimensional holes (Q2D) to three dimensional electrons (3D) for $SL_1$and also p type to n type conductivity respectively for SL_2.

In the investigated temperature range, the cut-off wavelength were ($3.92\ \mu m < \lambda_c < 5.92\ \mu m$) and ($5.06\ \mu m \leq \lambda_c \leq 6.30\ \mu m$) in the SL_1 and SL_2, respectively. These SL are medium infrared detectors (MWIR).

REFERENCES

[1] A.Rogalski, Infrared Detectors, Gordon and Breach Science Publishers, Amsterdam, 2000.
[2] P.R. Norton, Infrared detectors in the next millennium, Proc.SPIE 3698 (1999) 652–665.
[3] E. D. Palik, ed., Handbook of Optical Constants of Solids (Elsevier, 1998).
[4] D. L. Smith, C. Mailhiot, J. Phys. Rev. Lett. 58 (1987) 1264-1267.
[5] R. Dingle, A. C. Gossard, et W. Wiegmann, Direct Observation of Superlattice Formation in a SemiconductorHeterostructure, Phys. Rev. Lett. 34, 1327 - 1330 (1975).
[6] G. Bastard, Theoretical investigations of superlattice band structure in the envelope function approximation, Phys.Rev. B 25, 7584 – 7597 (1982).
[7] J. T. Cheung, G. Nizawa, J. Vac. Sci. Technol. A4(4), 101 (1986).
[8] G. Bastard, Phys., Rev. B 25 (1982) 7584–7597.
[9] G. Bastard, "Teoretical investigations of superlattice band structure in the envelope-function approximation" , Phys. Rev. B 25:7584, 1982.
[10] D. Barkissy, A. Nafidi, A. Boutramine, H. Charifi, A. Elanique, M. Massaq, "Electronic properties of GaAs/AlAs Nanostructure superlattice", J. Low Temp. Phys. 182-185, 2016.
[11] Boutramine, A. Nafidi, D. Barkissy, M. Bellioua, A. Khalal, Correlation between electronic bands structure and magneto-transport properties of nanostructure type II superlattice for terahertz detection, Superlattices and Microstructures, Volume 127, March 2019, Pages 151-156A.
[12] D. Barkissy, A. Nafidi, A. Boutramine, E. Y. El Yakoubi, H. Chaib, Investigations in electronic quantum transport of quasi two dimensional InxGa1-xAs/InP nanostructure superlattice for infrared detection, Superlattices and Microstructures, Volume 127, March 2019, Pages 54-60

International Journal of Engineering Research & Technology (IJERT)
ISSN: 2278-0181
Vol. 8 Issue 06, June-2019

[13] S. Perkowitz, R. Sudharsanan, K. A. Harris, J. W. Cook, Jr., J. F. Schetzina, and J. N. Schulman, "Effective mass in an n-type HgTe-CdTe superlattice", Journal Phys. Rev. B 36, 9290,1987.
[14] H.-S. Cho, "Density of states of quasi two one and zero dimensional superlattice", J. Vac. Sci. Technol. B Microelectron. Nanom. Struct. 7: 13-63, 1989.
[15] M. W. Prairie , R. M. Kolbas, " a general derivation of the density of states function for quantum wells and superlattices", Journal Superlattices and Microstructures, Vol. 7, No. 4, 1990.
[16] H.J. Haugan, S. Elhamri, B. Ullrich, F. Szmulowicz, G.J. Browna, W.C. Mitchel, J. Crys. Growth. (2009) 1897-1900.
[17] H.S. Jung, P. Boieriu, and C.H. Grein, "p-Type HgTe/CdTe Superlattices for Very-Long Wavelength Infrared Detectors", Journal of Electronic Materials vol. 35: no. 6, 1341–1345, 2006.